Evanescent Waves in PML's: Origin of the Numerical Reflection in Wave-Structure Interaction Problems

Jean-Pierre Bérenger

***Abstract*— The theory of general evanescent waves in perfectly matched layers (PML's) is presented, both in a continuous medium and in a discretized finite-difference medium. It is shown that evanescent waves may be strongly reflected from vacuum-PML interfaces in the discretized case. This allows the numerical reflection observed in wave-structure interaction problems to be interpreted as the reflection of evanescent fields surrounding the structures.**

***Index Terms*—Evanescent wave, FDTD, PML, reflection.**

I. Introduction

In many problems solved by means of finite methods (such as wave-structure interaction or microwave problems) evanescent fields are present in the region of interest. Since most of these problems are open ones, then requiring absorbing boundary conditions (ABC's) to absorb the outgoing fields, the behavior of evanescent waves in perfectly matched layers (PML's) is a question of prime importance in numerical electromagnetics. This question has been addressed or briefly mentioned in several papers [1]–[3] in the special case of waves whose direction of evanescence is perpendicular to the PML. In this paper, we consider more general evanescent waves having any direction of evanescence with respect to the PML. The behavior of such waves in PML's is investigated both in the theoretical continuous medium and in the discretized finite-difference time-domain (FDTD) medium.

The first part of the paper shows that general evanescent waves can exist in continuous PML's in which they are more absorbed than purely traveling waves. In theory such waves can penetrate into PML's without reflection from vacuum-PML interfaces. The second part of the paper investigates the behavior of evanescent waves in the discretized FDTD PML. Then, the properties of the PML may be quite different to the ones predicted in the continuous case. The theory of the numerical reflection especially shows that evanescent waves may be strongly reflected from vacuum-PML interfaces, resulting in important consequences to FDTD applications of PML's.

The last part of the paper is devoted to the interpretation of the spurious reflection observed in wave-structure interaction problems, which has been empirically investigated in [4], in view of optimizing the FDTD PML's. In the present paper, we show that the theory of the numerical reflection allows the characteristics of this reflection to be interpreted and reproduced. The conclusion is that the numerical reflection observed in wave-structure interactions clearly is due to the evanescent fields that surround the scattering structures.

Manuscript received February 11, 1999; revised July 21, 1999.

The author is with the Centre d'Analyse de Défense, Arcueil Cédex, 94114 France.

Publisher Item Identifier S 0018-926X(99)09379-5.

II. Evanescent Waves in a PML

As shown by Chew and Weedon [5], the dispersion relation in a PML medium is like in a vacuum, with just the wave numbers k_x, k_y, k_z divided by the stretching coefficients of the PML. In this paper, we consider only the two-dimensional (2-D) TE case, i.e., $k_z = 0$. The dispersion relation is

$$\frac{k_x^2}{s_x s_x^*} + \frac{k_y^2}{s_y s_y^*} = \frac{\omega^2}{c^2} \quad (\varepsilon\mu c^2 = 1) \tag{1}$$

where

$$s_u = 1 - j\frac{\sigma_u}{\varepsilon\omega}, \quad s_u^* = 1 - j\frac{\sigma_u^*}{\mu\omega} \quad (u = x, y) \tag{2}$$

in which σ quantities are the PML conductivities. In such papers as [5]–[7], only purely traveling waves have been considered, corresponding to part of the wave numbers that allow the 2-D dispersion relation (1), or its three-dimensional (3-D) counterpart, to be satisfied. In the present paper, we address more general solutions to (1), which yield nonuniform waves. In the 2-D TE case, for a waveform $\exp(j\omega t - jk_x x - jk_y y)$ at angular frequency ω, the PML equations [6] are

$$\varepsilon\omega s_y E_{x0} = -k_y H_{z0} \tag{3a}$$

$$\varepsilon\omega s_x E_{y0} = k_x H_{z0} \tag{3b}$$

$$\mu\omega s_x^* H_{zx0} = k_x E_{y0} \tag{3c}$$

$$\mu\omega s_y^* H_{zy0} = -k_y E_{x0} \tag{3d}$$

where $E_{x0}, E_{y0}, H_{z0} = H_{zx0} + H_{zy0}$ are the magnitudes of the components E_x, E_y, H_z. Obviously, this homogeneous system yields (1). As can be easily verified, the following wave numbers satisfy (1):

$$k_x = \frac{\omega}{c}\sqrt{s_x s_x^*}\,C(\chi,\theta) \tag{4a}$$

$$k_y = \frac{\omega}{c}\sqrt{s_y s_y^*}\,S(\chi,\theta) \tag{4b}$$

where

$$C(\chi,\theta) = \cosh\chi\cos\theta + j\sinh\chi\sin\theta \tag{5a}$$

$$S(\chi,\theta) = \cosh\chi\sin\theta - j\sinh\chi\cos\theta. \tag{5b}$$

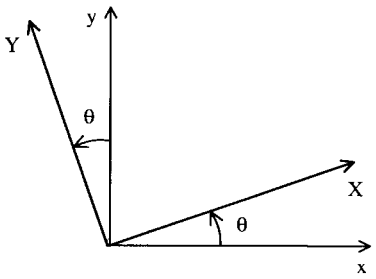

Fig. 1. System of coordinates (X, Y) forming an angle θ with system (x, y).

Other signs before the four terms in (5) also allow (1) to be satisfied. The set (5) has been arbitrarily selected among height possible solutions that would yield physically equivalent waves. Two special cases of (4) are well known. First, if $\cosh \chi = 1$ then $C = \cos\theta$ and $S = \sin\theta$, yielding traveling waves [6] propagating in direction θ with respect to the x axis. Second, if $\cos\theta = 1$ then $C = \cosh\chi$ and $S = -j \sinh\chi$, which corresponds to a wave propagating in x direction and evanescent in y direction, both in a vacuum [8] and in a PML [1]. The general solution (4), with any χ and θ, will yield nonuniform waves having any directions of propagation and evanescence with respect to the coordinate axis and then with respect to the PML which is perpendicular either to x or y axis. The field components corresponding to wave numbers (4) can be found from system (3) in the following form:

$$E_{x0} = -\sqrt{\frac{s_y^*}{s_y}} S(\chi,\theta) E_0 \tag{6a}$$

$$E_{y0} = \sqrt{\frac{s_x^*}{s_x}} C(\chi,\theta) E_0 \tag{6b}$$

$$H_{z0} = \sqrt{\frac{\varepsilon}{\mu}} E_0 \tag{6c}$$

$$H_{zx0} = H_{z0} C(\chi,\theta)^2 \tag{6d}$$

where E_0 is an arbitrary value homogeneous to an electric field. Equations (4) and (6) characterize a general nonuniform wave in a PML for the 2-D case considered in this paper.

Let us now assume that the PML is matched and perpendicular to x direction, with transverse conductivities equal to zero, i.e., $s_x = s_x^*$ and $s_y = s_y^* = 1$. From (4), any component of the wave is of the form

$$\psi = \psi_0 e^{j\omega[t - \frac{\cosh\chi}{c}(x\cos\theta + y\sin\theta) - \frac{\sigma_x}{\varepsilon c\omega}\sinh\chi\sin\theta x]} \times e^{-\frac{\omega}{c}\sinh\chi(y\cos\theta - x\sin\theta)} e^{-\frac{\sigma_x}{\varepsilon c}\cosh\chi\cos\theta x}. \tag{7}$$

By considering the (X, Y) system of coordinates forming an angle θ with respect to the (x, y) system (Fig. 1), (7) can be rewritten as

$$\psi = \psi_0 e^{j\omega[t - \frac{\cosh\chi}{c}X - \frac{\sigma_x}{\varepsilon c\omega}\sinh\chi\sin\theta x]} \times e^{-\frac{\omega}{c}\sinh\chi Y} e^{-\frac{\sigma_x}{\varepsilon c}\cosh\chi\cos\theta x} \tag{8}$$

where the exponential terms proportional to X and Y are exactly the corresponding terms of an evanescent wave propagating to $+X$ and decaying exponentially to $+Y$ in a vacuum. Two additional terms proportional to x and σ_x are present. First a phase term, second an absorbing term. With the change of coordinates corresponding to the rotation θ, the magnetic field (6) is left unchanged in (X, Y) coordinates while the electric field components become

$$E_{X0} = j\sinh\chi E_0 \tag{9a}$$

$$E_{Y0} = \cosh\chi E_0 \tag{9b}$$

which are nothing but the components of a wave propagating to $+X$ and evanescent to $+Y$ in a vacuum. Thus, in a PML perpendicular to x, i.e., if $\sigma_y = 0$, evanescent waves are as in a vacuum, with just the adjunction of phase and absorbing terms in the waveform. Especially, the magnitude of evanescent waves in PML's decays according to

$$|\psi_{\mathrm{PML}}| = |\psi_{\mathrm{vacuum}}| e^{-\frac{\sigma_x}{\varepsilon c}\cosh\chi\cos\theta x}. \tag{10}$$

Due to the parameter $\cosh\chi$, the absorbing coefficient in (10) differs from that of traveling waves. If $\cosh\chi = 1$ the wave is a purely traveling wave so that (10) holds as a special case traveling waves. What is important to be noticed is that evanescent waves are more absorbed than purely traveling waves, simply because $\cosh\chi > 1$. The more evanescent the wave (the larger $\cosh\chi$), the greater the absorption. If the directions of evanescence and propagation are perpendicular and parallel to the PML, respectively, $(\theta = \pm\pi/2)$, there is no absorption, as with traveling waves. This case has been addressed in [1] in view of waveguide applications of PML's. Equations (7)–(10) can be easily generalized to a PML with both σ_x and σ_y conductivities. Then, a second absorbing term is present in (10), with $\sigma_y, \sin\theta, y$, in place of $\sigma_x, \cos\theta, x$.

Let us now consider an interface between two PML's, with a nonuniform wave (4)–(6) propagating from medium 1 toward medium 2. The components of the wave vectors of the incident and transmitted waves must be equal in the interface, i.e., $k_{y1} = k_{y2}$. With (4b) and $\sigma_y = \sigma_y^* = 0$ in both media, this yields $S(\chi_2, \theta_2) = S(\chi_1, \theta_1)$. Similarly, the χ_r and θ_r parameters of the reflected wave must satisfy $S(\chi_r, \theta_r) = S(\chi_1, \theta_1)$. By solving for the unknowns χ and θ the equation $S(\chi, \theta) = S(\chi_1, \theta_1)$, which is equivalent to two real equations (real and imaginary parts), we obtain the following two solutions corresponding to the transmitted and reflected waves, respectively:

$$\chi_2 = \chi_1 \quad \theta_2 = \theta_1 \tag{11}$$

$$\chi_r = -\chi_1 \quad \theta_r = \pi - \theta_1. \tag{12}$$

Therefore, through PML-PML or vacuum-PML interfaces, the evanescence coefficient $\cosh\chi$ and the direction of propagation θ are left unchanged. The reflection coefficient can be found by enforcing the continuity of components E_y and H_z lying in the interface. Using (4), (6), (11), (12), we obtain the following relationships between the E_0 quantities of the incident, reflected, and transmitted waves:

$$E_{0i} - E_{0r} = E_{0t} \quad \frac{E_{0i}}{Z_i} + \frac{E_{0r}}{Z_r} = \frac{E_{0t}}{Z_t} \tag{13}$$

where Z_i, Z_r, Z_t are the ratios E_0/H_{z0} for the three waves. From (6-c) $Z_i = Z_r = Z_t$ so that (13) yields $E_{0r} = 0$.

In summary, evanescent waves from a vacuum can penetrate into a PML without reflection from the interface. In the PML such waves are absorbed according to the coefficient in (10). This absorption is added to the natural decrease of evanescent waves and is larger than the absorption of purely traveling waves.

III. Numerical Theory in a PML

This paragraph is devoted to the behavior of evanescent waves in the discretized FDTD medium, with a special emphasize on the reflection from vacuum-PML interfaces. Let us consider a wave of components $E_{x0}, E_{y0}, H_{zx0}, H_{zy0}$, with time and space variations as $\exp(j\omega t - j\bar{k}_x x - j\bar{k}_y y)$, where $\bar{k}_x$ and $\bar{k}_y$ are the wave numbers in the discretized medium. By enforcing this wave in the FDTD equations of the 2-D TE case [6], for a matched PML we obtain

$$\varepsilon\Sigma_y E_{x0} = -\frac{\Delta t}{\Delta y} B_y \sin\frac{\bar{k}_y \Delta y}{2} H_{z0} \tag{14a}$$

$$\varepsilon\Sigma_x E_{y0} = \frac{\Delta t}{\Delta x} B_x \sin\frac{\bar{k}_x \Delta x}{2} H_{z0} \tag{14b}$$

$$\mu\Sigma_x H_{zx0} = \frac{\Delta t}{\Delta x} B_x \sin\frac{\bar{k}_x \Delta x}{2} E_{y0} \tag{14c}$$

$$\mu\Sigma_y H_{zy0} = -\frac{\Delta t}{\Delta y} B_y \sin\frac{\bar{k}_y \Delta y}{2} E_{x0} \tag{14d}$$

where $\Delta x, \Delta y, \Delta t$ are the space and time steps and

$$A_u = e^{-\sigma_u \Delta t/\varepsilon} \quad B_u = \frac{\varepsilon(1-A_u)}{\sigma_u \Delta t} \quad (u = x, y) \tag{15}$$

$$\Sigma_u = \frac{e^{j\omega\Delta t/2} - A_u e^{-j\omega\Delta t/2}}{2j} \quad (u = x, y). \tag{16}$$

System (14) is analogous to (3) with the changes

$$k_u \to \frac{1}{\Delta u}\sin\frac{\bar{k}_u \Delta u}{2} \quad (u = x, y) \tag{17a}$$

$$s_u = s_u^* \to \frac{\Sigma_u}{\omega\Delta t}\frac{1}{B_u} \quad (u = x, y) \tag{17b}$$

so that the solutions of (3) give the solutions of (14). For instance, the equation of dispersion (1) is valid with changes (17) and (4) gives the wave numbers in the FDTD medium

$$\sin\frac{\bar{k}_x \Delta x}{2} = \frac{\Delta x}{c\Delta t}\Omega_x C(\chi, \theta) \tag{18a}$$

$$\sin\frac{\bar{k}_y \Delta y}{2} = \frac{\Delta y}{c\Delta t}\Omega_y S(\chi, \theta) \tag{18b}$$

where

$$\Omega_u = \frac{\Sigma_u}{B_u} \quad (u = x, y). \tag{19}$$

Notice that (18) yields (4) if the space and time steps vanish. The components (6) are also valid with the changes (17), so that the ratio E_0/H_{z0} equals the impedance of a vacuum—as in the continuous PML.

A. Reflection from a Vacuum-PML Interface

Let us now consider the transmission and reflection of a wave at a PML–PML interface, with uniform conductivities σ_{x1} and σ_{x2} in the PML's and σ_{x0} in the interface (Fig. 2). As in the continuous case, the $\bar{k}_y$ wave numbers must be equal.

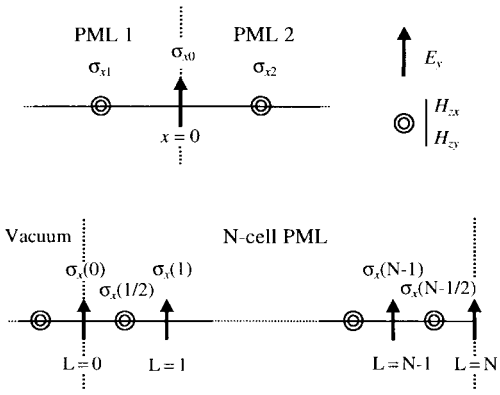

Fig. 2. Interface between two PML's with uniform conductivities (upper part) and between a vacuum and a N-cell-thick PML with nonuniform conductivity (lower part).

From (18b) this also yields (11) and (12). Defining R as the ratio of the reflected to the incident E fields in the interface, that is $E_{0r}C(\chi_r, \theta_r)/E_{0i}C(\chi_1, \theta_1) = -E_{0r}/E_{0i}$, and setting $x = 0$ in the interface, components E_y and H_z in medium 1 can be written as

$$E_{yi} + E_{yr} = E_{0i}C(\chi_1, \theta_1)[e^{-j\bar{k}_{x1}x} + Re^{j\bar{k}_{x1}x}]e^{j\omega t - j\bar{k}_{y1}y} \tag{20a}$$

$$H_{zi} + H_{zr} = \sqrt{\frac{\varepsilon}{\mu}}E_{0i}[e^{-j\bar{k}_{x1}x} - Re^{j\bar{k}_{x1}x}]e^{j\omega t - j\bar{k}_{y1}y}. \tag{20b}$$

In the FDTD procedure, the continuity of E_y is retained in the interface (E_y nodes) in which $E_{yi} + E_{yr} = E_{yt}$. From this, using (11) and (20) the transmitted wave can be written as

$$E_{yt} = (1+R)E_{0i}C(\chi_1, \theta_1)e^{j\omega t - j\bar{k}_{x2}x - j\bar{k}_{y1}y} \tag{21a}$$

$$H_{zt} = (1+R)\sqrt{\frac{\varepsilon}{\mu}}E_{0i}e^{j\omega t - j\bar{k}_{x2}x - j\bar{k}_{y1}y}. \tag{21b}$$

Inserting the above three waves into the FDTD equation of the interface [6], which involves $E_y(x = 0), H_z(x = -\Delta x/2), H_z(x = \Delta x/2)$, we obtain

$$\begin{aligned}(1+R)C(\chi_1, \theta_1)e^{j\omega\Delta t/2} &= A_{x0}(1+R)C(\chi_1, \theta_1)e^{-j\omega\Delta t/2} \\ &\quad - \frac{\Delta t}{\sqrt{\varepsilon\mu}\Delta x}B_{x0}[(1+R)e^{-j\bar{k}_{x2}\Delta x/2} \\ &\quad - (e^{j\bar{k}_{x1}\Delta x/2} - Re^{-j\bar{k}_{x1}\Delta x/2})].\end{aligned} \tag{22}$$

By solving for R and eliminating the exponentials on $\bar{k}_x$ using (18a), the reflection coefficient at a PML-PML interface is then

$$R = -\frac{2j\Omega_{x0} + \Lambda_{x2} - j\Omega_{x2} - \Lambda_{x1} - j\Omega_{x1}}{2j\Omega_{x0} + \Lambda_{x2} - j\Omega_{x2} + \Lambda_{x1} - j\Omega_{x1}} \tag{23a}$$

where

$$\Lambda_{xi} = \sqrt{\frac{1}{C(\chi_1, \theta_1)^2}\frac{c^2\Delta t^2}{\Delta x^2} - \Omega_{xi}^2}. \tag{23b}$$

Notice that R depends on the conductivities $\sigma_{x1}, \sigma_{x2}, \sigma_{x0}$ through $\Omega_{x1}, \Omega_{x2}, \Omega_{x0}$. As can be shown, (23) holds as a

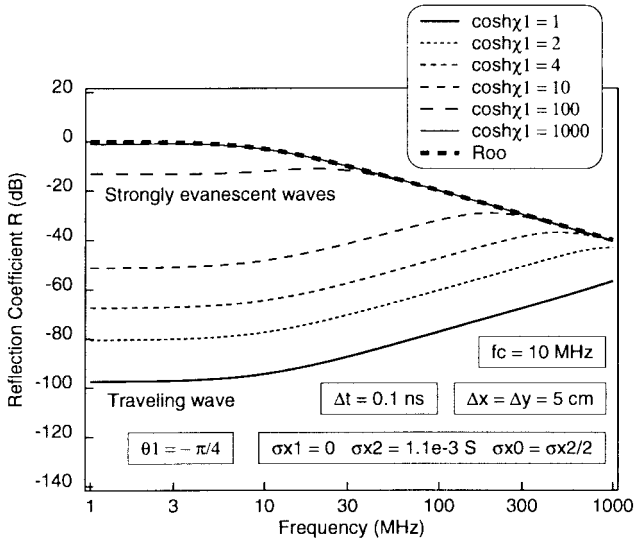

Fig. 3. Numerical reflection from an interface located between a vacuum and an infinite PML for various values of the evanescence parameter $\cosh\chi_1$.

special case $(C = \cos\theta_1)$ the reflection coefficient given in [2] and [3].

An important simplification of (23) is obtained in the case when the parameter $\cosh\chi_1$ of the incident wave is large (strongly evanescent wave). By assuming that $\omega\Delta t \ll 1$ and $\sigma_x\Delta t/\varepsilon \ll 1$ for all the conductivities, two assumptions that usually hold in PML's, at a vacuum-PML interface $(\sigma_{x1} = 0)$ the limit of R as $\cosh\chi_1$ tends to infinity can be derived as

$$R_\infty = \frac{j\sigma_{x0}/\varepsilon\omega}{1 - j\sigma_{x0}/\varepsilon\omega}. \tag{24}$$

An example of reflection R from (23) is shown in Fig. 3, for the incidence $\theta_1 = -\pi/4$ and $\cosh\chi_1$ in the range 1–1000. Notice that θ_1 is negative in order that the incident wave is evanescent toward the PML [for a given physical problem, the sign of θ depends on the choice of the signs in (5)]. From traveling waves $(\cosh\chi_1 = 1)$ to strongly evanescent waves (large values of $\cosh\chi_1$), R grows up to R_∞. In accordance with (24), the strongly evanescent waves are totally reflected $(R = -1)$ at frequencies far smaller than cutoff

$$f_c = \frac{\sigma_{x0}}{2\pi\varepsilon}. \tag{25}$$

For a vacuum-PML interface, with σ_{x0} of the order of σ_{x2} (say $\sigma_{x0} = \sigma_{x2}$ or $\sigma_{x0} = \sigma_{x2}/2$), one can easily show that R is close to its limit R_∞ for $f \ll fc$, as long as

$$\cosh\chi_1 \gg \frac{2c\varepsilon}{\sigma_{x2}\Delta x}. \tag{26}$$

Condition (26) can be interpreted by considering the absorption coefficient in (10). Since $\chi_2 = \chi_1$ from (11), if (26) holds the evanescent wave transmitted into the PML must be totally absorbed upon a range shorter than the FDTD cell size Δx, i.e., within one cell. This cannot be achieved, resulting in a strong numerical reflection. As can be seen in Fig. 3 and predicted by theory, at $f > f_c$ smaller values of $\cosh\chi_1$ make R_∞ valid.

B. Reflection from an N-Cell-Thick PML

We now consider an incident wave of parameters $\bar{k}_{y1}, \chi_1, \theta_1$, and a PML of N cells in thickness with a nonuniform conductivity, i.e., a conductivity depending on the mesh index L (Fig. 2). The wave transmitted into the PML is of the form (6) and at each interface $\bar{k}_y, \chi, \theta$ are left unchanged, so that $\bar{k}_y = \bar{k}_{y1}$, $\chi = \chi_1$, and $\theta = \theta_1$, in the whole of the PML. The incident and reflected waves can be written as with a single interface (20). Denoting by $T(L)$ unknowns quantities at rows L, let the electric field E_y be written as

$$E_y(L) = E_{0i}T(L)C(\chi_1,\theta_1)e^{j\omega t - j\bar{k}_{y1}y} \qquad (L = 1,\cdots,N-1). \tag{27}$$

Similarly, at rows $L + 1/2$, using (6) let the magnetic field be written as

$$H_z(L+1/2) = \sqrt{\frac{\varepsilon}{\mu}}E_{0i}T(L+1/2)e^{j\omega t - j\bar{k}_{y1}y} \qquad (L = 0,\cdots,N-1) \tag{28a}$$

$$H_{zx}(L+1/2) = C(\chi_1,\theta_1)^2 H_z(L+1/2) \qquad (L = 0,\cdots,N-1). \tag{28b}$$

Finally, at the end of the PML

$$E_y(N) = 0. \tag{29}$$

Inserting (20) and (27)–(29) into the N FDTD equations of the advance on time of E_y and into the N equations of the advance of H_{zx}, from $L = 0$ to $L = N-1$, we obtain a set of $2N$ equations for the $2N$ unknowns $R, T(1/2), \cdots, T(N-1/2)$. After eliminating the incident wave number with (18a), this set can be written in the form

$$M \cdot \begin{pmatrix} R \\ T(1/2) \\ T(1) \\ \vdots \\ T(N-1/2) \end{pmatrix} = \begin{pmatrix} V \\ \alpha D(1/2) \\ 0 \\ \vdots \\ 0 \end{pmatrix} \tag{30}$$

where M is the tridiagonal matrix

$$M = \begin{pmatrix} U & \alpha D(0) & \cdots & & \\ \cdots & \cdots & \cdots & & \\ \cdots & -\alpha D(L) & 1 & \alpha D(L) & \cdots \\ \cdots & -\alpha D\left(L+\frac{1}{2}\right) & 1 & \alpha D\left(L+\frac{1}{2}\right) & \cdots \\ & \cdots & \cdots & \cdots & \\ & & \cdots & -\alpha D\left(N-\frac{1}{2}\right) & 1 \end{pmatrix}$$

and

$$\alpha = \frac{c\Delta t}{\Delta x}\frac{1}{C(\chi_1,\theta_1)}; \quad D(L) = \frac{1}{2j\Omega_x(L)}$$

$$U = 1 + \alpha D(0)[\sqrt{1-Q^2} - jQ]; \quad Q = \frac{1}{\alpha}\sin\frac{\omega\Delta t}{2}$$

$$V = -1 + \alpha D(0)[\sqrt{1-Q^2} + jQ].$$

System (30) can be solved recursively for the unknown of interest R. For strongly evanescent waves, i.e., if $\cosh\chi_1$ is large enough, α vanishes and (30) also yields the limit R_∞ (24) with validity condition (26) for $f \ll f_c$, with just $\sigma_x(L = 0)$ in place of σ_{x0} and σ_{x2} in (24) and (26).

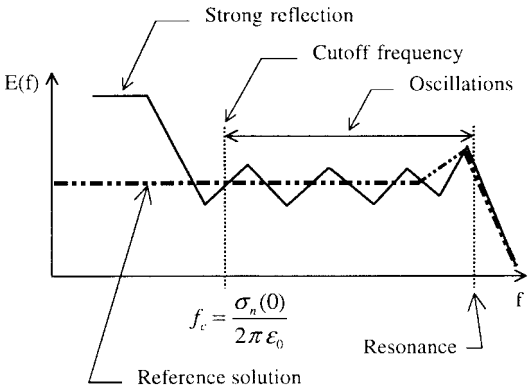

Fig. 4. Typical shape of the normal electric field on the surface of a scattering structure surrounded by a close PML.

IV. Interpretation of the Numerical Reflection in Wave-Structure Interaction Problems

Wave-structure interaction problems are important applications of numerical methods, in the fields of electromagnetic compatibility (EMC) and radar cross section (RCS) calculations. To compute acceptable results, it is known that such ABC's as the one-way wave equation or the matched layer must be set some distance from the scattering structure. In general, the required distance is at least equal to half the length of the structure. As early as the initial FDTD tests with the PML method, it appeared that a similar condition holds if the PML is thin, for instance thinner than five FDTD cells, but does not hold with a thick PML. In the last case, the PML can be set quite close to the structure, as close as two FDTD cells, resulting in a wide reduction of the computational domain.

The reflection observed with short structure-PML separations has been heuristically analyzed in [4], resulting in an optimum profile of conductivity whose parameters have been found empirically. In all the interaction problems, the frequency-domain electric field on the surface of a scatterer surrounded by a close PML is shaped as in Fig. 4. This shape is very pronounced with simple scatterers as plates, especially in 2-D cases, but is always visible, even with complex 3-D structures. Below a certain frequency f_c, depending on the conductivity implemented in the vacuum-PML interface $\sigma_n(0)$, a strong reflection is observed, i.e., the results strongly depart from the reference solution computed with a PML or any ABC set far away from the scatterer. From f_c to the resonance frequency of the structure, the results oscillate about the reference solution. And above the resonance frequency, no significant numerical reflection is present.

Frequency f_c in Fig. 4 was first found by means of experiments such as the ones in [4]. Now, we notice that this frequency is exactly the cutoff (25) of the numerical reflection of strongly evanescent fields from vacuum-PML interfaces. Therefore, it is clear that the reflection below f_c is due to strongly evanescent waves whose $\cosh\chi$ satisfy (26), i.e., waves that must be absorbed, in theory, within one FDTD cell. We show below that the oscillatory reflection also is due to the evanescent fields surrounding the scattering structures.

To interpret the oscillatory reflection, we should have an order of magnitude of the parameter $\cosh\chi$ of the evanescent waves surrounding the scatterer. Let us consider a scatterer whose largest size is w. In the surrounding space, the evanescent fields decay as

$$e^{-\frac{\omega}{c}\sinh\chi d} \tag{31}$$

where d is the distance from the scatterer. At a distance of the order of the size w, these fields are negligible or at least small. This can be written as

$$e^{-\frac{\omega}{c}\sinh\chi w} = e^{-p} \tag{32}$$

where p could be in the range 1–4 corresponding to coefficient (32) between 0.36 and 0.02. For our purpose, the exact value of p is of little importance. What is important is the frequency dependence of $\cosh\chi$. From (32) we obtain

$$\cosh\chi = \sqrt{1+\frac{p^2c^2}{\omega^2w^2}} \tag{33}$$

which shows that $\cosh\chi$ is close to unity at the resonance frequency of the scatterer $\omega = \pi c/w$, for instance in the range 1.05–1.6 with p in 1–4. Finally, let (33) be rewritten as

$$\cosh\chi = \sqrt{1+\frac{(\cosh^2\chi_0 - 1)f_0^2}{f^2}} \tag{34}$$

where $\cosh\chi_0$ is the value of $\cosh\chi$ at the resonance frequency f_0. Notice that the frequency dependence of $\cosh\chi$ is like in a waveguide.

An example of calculation of reflection R with (30) and (34) is shown in Fig. 5, for a PML(4-G10-1), i.e., a four-cell-thick PML with a geometrical conductivity [4] of ratio 10 and a normal reflection of 1%. The FDTD cell size is 5 cm, frequency $f_0 = 150$ MHz, $\cosh\chi_0 = 1.1$ (corresponding to $p \approx 1.4$), and the incidence θ is either -45 or $-75°$. The upper part shows $\cosh\chi$ as a function of frequency, the middle two parts the modulus and phase of R, and the lower part quantity $1-R$. At low frequencies, $\cosh\chi$ is large, (26) holds, frequency is lower than f_c (25), so that R is large in accordance with (24). Around and above f_c, R is smaller but not negligible. Its phase quickly varies in this region. As frequency grows the reflection is mainly due to either an electric or a magnetic conductivity, resulting in a rotating phase of the reflection. As a result, quantity $1-R$ oscillates between $1-|R|$ and $1+|R|$. We observe that $1-R$ in Fig. 5 is shaped as the FDTD results [4] summarized in Fig. 4. This strongly suggests that the numerical reflection observed above f_c is due to the reflection of evanescent fields from the PML. In other words, the result computed on the surface of a scatterer is the sum of the exact field with evanescent fields reflected from the PML. Notice that the period of the rotation of the phase of R, and then the period of the oscillations of $1-R$, corresponds to a ratio of frequencies equal to the ratio of successive conductivities in the PML, i.e., the ratio of the geometrical profile of conductivity (ratio of 10 in Fig. 5).

Fig. 6 shows an attempt to reconstructing a FDTD result in [4] by means of both the theoretical numerical reflection (30) and assumption (34). The upper part from [4] gives the normal electric field on a 2-D 20-cell-thin plate surrounded by various four-cell PML's set two cells from the plate. The lower part

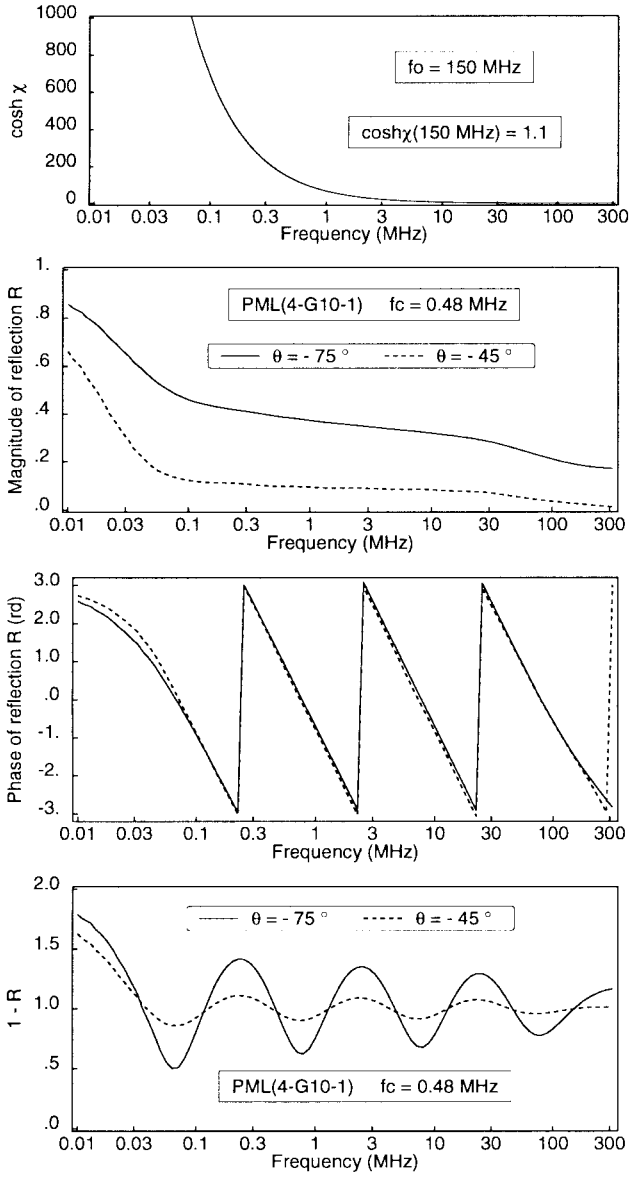

Fig. 5. Numerical reflection from a four-cell-thick PML with a geometrical conductivity. The FDTD steps are $\Delta x = \Delta y = 0.5$ cm and $\Delta t = 0.1$ ns.

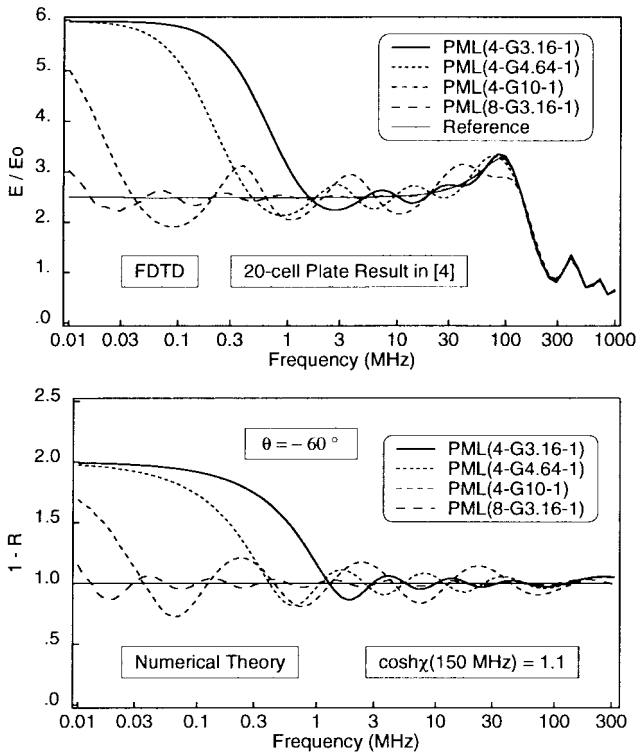

Fig. 6. An attempt to reconstructing the normal field computed with the FDTD method at the end of a 20-cell-thin plate [4]. The FDTD steps are $\Delta x = \Delta y = 0.5$ cm and $\Delta t = 0.1$ ns.

shows quantity $1-R$ computed by (30) and (34) for the same four PML's as in the FDTD calculation, at incidence $-60°$. The oscillatory region is like that of the FDTD result. Only the magnitude of the oscillations would be modified by changing the incidence θ (see Figs. 5 and 7). The low-frequency plateau also is like its FDTD counterpart, although its magnitude, which does not depend on θ ($R = -1$ in this region), is lower than the FDTD one. Such a difference in the magnitudes of the plateaus is due to the fact that the field between the scatterer and the PML is not simply $1-R$. There are multiple reflections between the two reflecting surfaces. With an infinite plate and an infinite PML, the normal electric field would be the sum of contributions proportional to $1, -2R, 2R^2, -2R^3, \cdots$, resulting in a field tending to infinity at low frequencies where R tends to -1. Actually, the cavity formed by the scatterer and the PML is not without losses, so that the ratio of the plateau to the reference solution is finite. This ratio is only 2.5 in Fig. 6, but it may be far greater depending on the scatterer and the location on it. As an example, a ratio of 5 can be seen in [9] on a 100-cell plate. In the oscillatory region, the effect of terms $R^2, R^3, \cdots$ is small or negligible since R is small (Fig. 5), so that the magnitude of the oscillations is less dependent on the scatterer and location of interest. Finally, although a little arbitrary parameters such as $\cosh \chi_0$ are of concern, the theory of numerical reflection allows all the characteristics of the FDTD results to be well reconstructed and interpreted. This clearly demonstrates that the spurious reflection in interaction problems is due to evanescent fields with frequency dependence like (34).

Although quantity $1-R$ cannot accurately predict the field on a scatterer, it is well representative of what can be expected in the oscillatory region, which is the main region of interest as making use of PML's. Fig. 7 compares $1-R$ for various incidences and three PML's. The first two PML's are four and eight cell thick, with geometrical profiles of ratios 10 and 3.16, respectively. As observed in [4], the oscillations above f_c can be reduced by decreasing the ratio of successive conductivities. This reduction is more important at medium incidences (30–75°) than at grazing incidence. The lower part of Fig. 7 was computed with the modified PML presented in [9], denoted by PML-D, which is based on an additional splitting of the subcomponents in the PML. The theoretical reflection from such a PML-D is a generalization of (30) which can be found in [10]. As demonstrated by comparing the upper and lower parts in Fig. 7, the reflection in the oscillatory region is dramatically reduced by substituting PML-D to PML, especially at high-incidence angles. PML-D

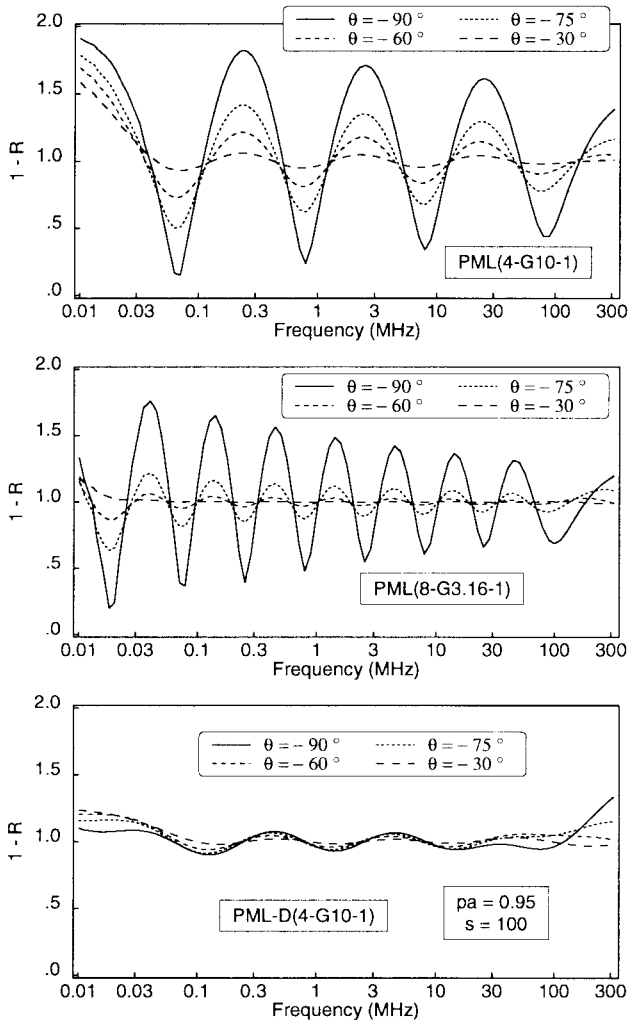

Fig. 7. Comparison of the numerical reflection of two PML's with the numerical reflection of the modified version PML-D [9]. Parameters p_a and s are defined in [9]. The FDTD steps are $\Delta x = \Delta y = 0.5$ cm and $\Delta t = 0.1$ ns.

is very well suited to problems involving evanescent fields at grazing incidence, as illustrated with waveguides in [10]. In wave-structure interactions, the incidences are smaller so that the interest of PML-D seems lesser. Actually, in terms of computational cost, the best choice for a given level of reflection, either PML or PML-D, depends on such parameters as the duration of the calculation or the frequency bandwidth of interest. For a given problem, comparisons as the one in Fig. 7 could help users in selecting the best PML.

V. Conclusion

In theory, evanescent waves are more absorbed than traveling waves in PML's, without reflection from vacuum-PML interfaces. Actually, in the discretized FDTD medium things may be quite different, an important or even total reflection occurs from PML's at some frequencies. This reflection results from the rate of decay of the evanescent fields in the PML's, which may be so strong that it cannot be properly sampled by the FDTD mesh. As a consequence, a similar reflection is also expected with other finite methods that discretize space [11].

The spurious reflection observed in wave-structure interaction problems [4] can be clearly interpreted by means of the numerical theory. This reflection is due to the strongly evanescent fields that surround the structures, which are, in part or in totality, reflected from the FDTD PML's.

References

[1] J. De Moerloose and M. A. Stuchly, "Behavior of Bérenger's ABC for evanescent waves," *IEEE Microwave Guided Wave Lett.*, vol. 5, pp. 344–346, Oct. 1995.
[2] W. C. Chew and J. M. Jin, "Perfectly matched layers in the discretized space: An analysis and optimization," *Electromagn.*, vol. 16, no. 4, pp. 325–340, July 1996.
[3] J. Fang and Z. Wu, "Closed form expression of numerical reflection coefficient at PML interfaces and optimization of PML performance," *IEEE Microwave Guided Wave Lett.*, vol. 6, pp. 332–334, Sept. 1996.
[4] J.-P. Bérenger, "Perfectly matched layer for the FDTD solution of wave-structure interaction problems," *IEEE Trans. Antennas Propagat.*, vol. 44, pp. 110–117, Jan. 1996.
[5] W. C. Chew and W. H. Weedon, "A 3-D perfectly matched medium from modified Maxwell's equations with stretched coordinates," *IEEE Microwave Opt. Tech. Lett.*, vol. 7, pp. 599–604, Sept. 1994.
[6] J.-P. Bérenger, "A perfectly matched layer for the absorption of electromagnetic waves," *J. Comput. Phys.*, vol. 114, pp. 185–200, Oct. 1994.
[7] ———, "Three-dimensional perfectly matched layer for the absorption of electromagnetic waves," *J. Comput. Phys.*, vol. 127, pp. 363–379, Sept. 1996.
[8] J. A. Kong, *Theory of Electromagnetic Waves*. New York: Wiley, 1975.
[9] J.-P. Bérenger, "Improved PML for the FDTD solution of wave-structure interaction problems," *IEEE Trans. Antennas Propagat.*, vol. 45, pp. 466–473, Mar. 1997.
[10] ———, "An effective PML for the absorption of evanescent waves in waveguides," *IEEE Microwave Guided Wave Lett.*, vol. 8, pp. 188–190, May 1998.
[11] ———, "Numerical reflection of evanescent waves by PMLs: Origin and interpretation in the FDTD case—Expected consequences to other finite methods," *Int. J. Num. Modeling*, to be published.

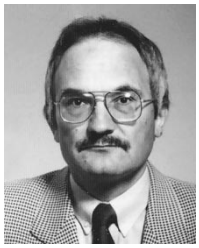

Jean-Pierre Bérenger received the Maîtrise de Physique degree from Université de Grenoble, France, in 1973, and the Diplôme d'Ingénieur degree from Ecole Supérieure d'Optique de Paris, France, in 1975.

From 1975 to 1984, he was with the Département Etudes Théoriques, Centre d'Analyse de Défense, where his domains of interest were the propagation of waves and the coupling problems related to the nuclear electromagnetic pulse. During this period he helped popularize the finite-difference time-domain method in France. In 1984 he moved to the Département Nucléaire where he was involved in the development of simulation software. From 1989 to 1998 he held a position as expert on the electromagnetic effects of nuclear disturbances. He is now a Contract Manager while staying active in the field of numerical electromagnetics.